

NACA TM 1326



DEC 12 1951

NATIONAL ADVISORY COMMITTEE FOR AERONAUTICS

TECHNICAL MEMORANDUM 1326

CONCERNING THE FLOW ABOUT RING-SHAPED COWLINGS
PART II - ANNULAR BODIES OF INFINITE LENGTH
WITH CIRCULATION FOR SMOOTH ENTRANCE

By Dietrich Küchemann and Johanna Weber

Translation of ZWB Forschungsbericht Nr. 1236/2, Nov. 11, 1940



Washington

November 1951

NACA LIBRARY
LANGLEY AIRCRAFT RESEARCH CENTER
Hampton, Va.



NATIONAL ADVISORY COMMITTEE FOR AERONAUTICS

TECHNICAL MEMORANDUM 1326

CONCERNING THE FLOW ABOUT RING-SHAPED COWLINGS

PART II - ANNULAR BODIES OF INFINITE LENGTH

WITH CIRCULATION FOR SMOOTH ENTRANCE*

By Dietrich Küchemann and Johanna Weber

ABSTRACT:

The investigations carried out in a previous report (reference 1) concerning the flow about ring-shaped cowlings were extended by taking a circulation about the cowling into consideration. The present second report treats bodies of infinite length with approximately smooth entrance. The circulation was caused by distributing vortexrings of constant density over a stream surface extending to infinity. Furthermore, the influence of a hub body on such cowlings was dealt with. The examples treated are meant to give to the designer a basis for his design.

OUTLINE:

- I. STATEMENT OF THE PROBLEM AND METHOD
- II. RESULTS
 - 1. Annular Bodies without Hub
 - 2. The Influence of a Hub Body as Seen in the Example of Annular Bodies without Circulation
 - 3. Annular Bodies with Hub
 - 4. Mass Flows and Thrust Forces
- III. SUMMARY
- IV. REFERENCES

I. STATEMENT OF THE PROBLEM AND METHOD

In the first of this series of reports concerning the flow about ring-shaped cowlings of finite thickness (reference 1), it was shown how to obtain in a simple manner the forms and pressure distributions of ring-shaped bodies from existing tables of functions according to the customary

*"Über die Strömung an ringförmigen Verkleidungen. II. Mitteilung: Ringkörper unendlicher Tiefe mit Zirkulation bei stossfreiem Eintritt." Zentrale für wissenschaftliches Berichtswesen über Luftfahrtforschung des Generalluftzeugmeisters (ZWB) Berlin-Adlershof, Forschungsbericht Nr. 1236/2, Göttingen, Nov. 11, 1940.

method of superposition of flow due to singularities and parallel flow. Whereas in reference 1, a circulation about the cowling - which would cause a velocity in the interior of the ring different from that in the exterior - was not considered, the present report will deal especially with the influence of such a circulation. We shall, however, limit ourselves to cowlings of infinite length and, thus, obtain an insight as to the flow conditions about such cowlings for smooth entrance. We herein utilize the advantage of the singularity method of yielding body shapes and velocities, which in the case of given singularities is relatively simple. However, the inverse problem - determining the singularities for a given body shape or velocity distribution - is considerably more difficult and troublesome. We hope to be able later on to treat arbitrary bodies of finite length with circulation for non-smooth entrance as well.

In the present report, the starting point is simple singularities. It will be shown that even the simplest singularities yield shapes and pressure distributions that are absolutely usable in practice. Moreover, it will be possible to recognize fundamentally, for instance, the influence of a hub body; however, it must again be stressed that we obtain cowlings which the flow always approaches in the most favorable manner only (approximately smooth entrance), and that we do not investigate a certain form for various operating conditions. The examples described are meant, above all, to give the designer a basis for the design of aerodynamically favorable ring-shaped cowlings.

We shall first discuss the singularities.

We obtained a thick ring-shaped body in the simplest manner by placing a source ring into a given main flow. For the bodies of infinite length treated here, one such source ring will be sufficient. The simplest main flow is the parallel flow. We then obtain the annular bodies without circulation treated in reference 1. A hub body is produced by placing a three-dimensional single source on the symmetry axis. Finally, a main flow with different velocities within and outside of a ring is obtained by distributing vortices over a stream surface. We select vortex rings, the centers of which lie on the symmetry axis. Since we want to investigate the entrance, the distribution must start at a certain point and may extend to infinity. It will be shown that it is sufficient to assume the density of the distribution constant in the direction of the symmetry axis. For the numerical calculation, the values of the stream function and velocity components of source and vortex ring are taken from the tables of functions (reference 2) where the pertinent formulas also are to be found. The accuracy of the calculations corresponds to the slide-rule accuracy.

In view of the great number of parameters, we must necessarily limit ourselves to a few characteristic values. The thickness d of the

cowling (compare fig. 1) is referred to the radius R at the infinity of the streamline on which lies the source ring, and all results are given only for the values $d/R = 0$ (mean camber stream surface) and 0.2. Intermediate values may be linearly interpolated. The radius R_N of the hub body is accordingly referred to the radius r_0 of the source ring by which the distance a in axial direction between source ring and single source on the axis also is standardized. The shapes and pressure distributions are indicated, in general, for the values $R_N/r_0 = 0, 2/3, 1$, and $a/r_0 = 0, 0.5, 1$. We characterized the strength of the circulation by the ratio between the velocity U_∞ which ultimately results within the ring and the undisturbed velocity of the oncoming flow U_0 in the outer space, and assume the values U_∞/U_0 as 0.2, 0.4, 0.6, 0.8, 1.0, and in a few cases up to 2.0.

II. RESULTS

1. Annular Bodies without Hub

We investigated, first, annular bodies with circulation without hub. We have already noted that we want to produce the velocity differences by a constant distribution of vortex rings over a stream surface. The shape of this stream surface is unknown at first. If, for instance, an axially parallel cylinder with a distribution of vortex rings is put into a flow in the direction of the axis, the cylinder does not remain a stream surface. The originating streamline pattern is drawn in dashed lines in figure 2. An iteration method can be carried out by placing the distribution on that stream surface which has the same starting point ($x = 0$; $r = r_0$). Step by step, we thus approach the stream surface which coincides with the locus of the distribution for the prescribed vortex strength. Figure 2 shows the result (U_∞/U_0 about 0.3) in the solidly drawn streamlines. The position of the distribution is heavily outlined. It could be made the wall and would be stream surface when the prescribed velocity ratio is produced. From this consideration it follows that a certain wall is obtained for each velocity ratio. These walls are plotted for various U_∞/U_0 in figure 3. For $U_\infty/U_0 = 1$ naturally a cylinder results (no circulation). For values smaller than 1, the walls are bent inward toward the front; for values larger than 1, they are bent outward.

The originating flow conditions are of interest. In figures 4 and 5, we plotted once more the velocity components of the vortex flow alone (at the same time as illustration of the dashed-line streamline pattern, fig. 2) for the case that the distribution is located on a cylinder. We can see that very soon parallel flow, stemming from the

vortices, develops in the interior of the ring. The corresponding figures for the case where the distribution is a stream surface have not been drawn again. The deviations may be understood with the aid of figure 2. Figure 5 shows, furthermore, that the vortices at the initial point of the distribution ($x = 0$; $r = r_0$) cause an infinitely high radial velocity.¹ Our simple assumption becomes noticeable in the streamline pattern by a vertical inflectional tangent of the respective streamline at this point; however, this fact cannot be expressed in the diagram. Since, furthermore, such cowlings in practice always will be of finite thickness, this singular point remains without decisive influence. If later on in the pressure distributions at this point, an infinity appears for $d = 0$ and a local suction peak for $d \neq 0$, this, too, is caused by the simplification mentioned. Nevertheless, refinement of the theory in the manner indicated above was foregone since its effects are immediately clear and we are here concerned only with fundamentals.

The continuity equation readily gives information about the mean velocities in any cross section within the ring, since cross-sectional area and velocity at infinity are known. Accordingly, the ratio between the mean velocity U in the entrance cross section ($x = 0$) and U_0 is plotted against the velocity ratio in figure 6. This quantity also represents the ratio between the quantity of fluid flowing in the interior of the ring in the presence of circulation, and the quantity which would flow through the entrance cross section without circulation; thus, the ratio $Q_0 = \pi r_0^2 U_0$. The mean velocity U in the entrance cross section is therewith shown to be not yet the final velocity U_∞ ; however, if one proceeds somewhat further into the cowling ($x/R = 0.5$), the mean velocity has come considerably closer to the ultimate one, as figure 6 shows. The end velocity is attained to the same degree as the curves in figure 3 approach the asymptote. In figure 6, the contraction ratio r_0/R is plotted once again more accurately. Moreover, one recognizes from this figure that the velocity decrease or increase as well as the pressure recovery takes place neither completely inside nor completely outside of the cowling, so that one is dealing neither with a nose inlet nor with a side inlet according to P. Ruden (reference 3) but with an intermediate form. More accurate information can be gained from figure 7 where the pressure on the symmetry axis is plotted for $U_\infty/U_0 = 0.2$. For comparison, we see the pressure which would be caused by a vortex distribution over a cylinder. One recognizes that the pressure recovery takes place mainly ahead of the cowling so that one

¹In order to avoid this, the distribution would have to start as \sqrt{x} , for instance, as $\sqrt{x/r_0 + x}$. For the sake of the simplicity of the calculations, a constant vortex distribution was maintained.

may count on relatively small losses inside of the cowling. From figure 8, we can see the pressure at the cowling itself for the different velocity ratios. The appearance of an infinitely large pressure at the leading edge has already been discussed. Further inside, however, a very favorable pressure variation becomes evident which is caused by the constriction or extension, respectively, of the stream surface of the distribution. Thereby, one may subsequently justify the selection of the special vortex distribution.

If one now places into this basic flow a source ring at the start of the distribution, one obtains body shapes as indicated in figure 9. The source strength is determined in such a manner that a thickness of $0.2R$ results at infinity. One obtains, corresponding to the various mean camber lines (fig. 3), a certain body shape for each velocity ratio. In order to calculate the behavior of a certain body, for instance that of $U_\infty/U = 0.4$ in case of other velocities, one would have to determine the additional source and vortex ring distributions which make the prescribed body again a streamline; this calculation would exceed the scope of the present report.² Since the body shapes are, however, not too different, it may be assumed that the permissible velocity range for a certain form will not be too small. Figure 10 also shows the bodies of the thickness $d/R = 0.1$ for several velocity ratios and simultaneously, the mean camber streamline (dashed) from which one may see the position of the body contour with respect to the mean camber line. It is noteworthy that the inward curving of the mean camber line near the entrance opening is filled up by the source fluid so that a relatively straight body inside results.

The velocity and pressure distributions at the surface of these bodies have not been calculated. One may attain an approximate idea by superimposing the velocity distributions of annular source bodies without circulation ($U_\infty/U_0 = 1$, compare also fig. 13) resulting from the first report (reference 1) on those on the mean camber lines (fig. 8).

2. The Influence of a Hub Body as Seen in the Example of Annular Bodies without Circulation

It was shown in the first report what important effect a hub body may have on the flow conditions at the cowling. It could be shown that it is possible to attain, by favorable selection of position and thickness of the hub body, the absence of suction peaks, and only very slight incremental velocities for the pressure distributions at the inside and outside of the cowling. The radius R_H/r_0 and the position a/r_0 of the hub, being the most influential parameters in this respect, will be

²Compare section I.

treated first in somewhat more detail than in the first report (in this section without taking a circulation into consideration). The influence of circulation is investigated in section II, 3.

Figures 11 and 12 show the investigated forms of hub and cowling, partly to be found in the first report. The considerable thickening at the leading edge of the annular source body for $R_N/r_0 = 1$ and $a/r_0 = 1$ is noteworthy. Figures 13 to 18 show the pertaining pressure distributions on the surface of the cowlings. Figure 13 may be used as comparison for $R_N = 0$. The influence of the hub is shown particularly clearly by the pressure distribution on the mean camber line $d = 0$. Let us consider first the hub bodies of the radius $R_N/r_0 = 2/3$ in their various positions (figs. 14 to 16). No essential changes in pressure distribution are caused by a hub body of this thickness. The maximum negative pressures stay within moderate limits, and the maximum incremental velocities fluctuate between the values $0.16U_0$ and $0.25U_0$. The pressure distribution over the forms investigated shows the smallest incremental velocities and the smallest pressure rise for the value $a/r_0 = 0.5$. The thicker hub body $R_N/r_0 = 1$ (note the curves for $d = 0$) has considerably greater effort. For $a/r_0 = 0.5$ we have, for $d/R = 0.2$, no longer a suction peak on the inside of the cowling and only slight incremental velocities; for $a/r_0 = 1$, we have the same favorable conditions also on the outside of the cowling. A hub of this position and thickness obviously exerts a favorable influence on the flow at the cowling.

The pressure distributions on the hub body itself are plotted in figures 19 to 23. The cowling always affects the hub in an unfavorable sense though only to a small extent. The position $a/r_0 = 0.5$ is again shown to be a favorable position for $R_N/r_0 = 2/3$, just as is the position $a/r_0 = 1$, recognized as favorable before for $d/r_0 = 1$.

The examples of this section have once more demonstrated in detail what effect a hub may have on the flow at the cowlings. It must be noted, though, that no statement can be made on the behavior of these bodies if the oncoming flow is not smooth.

3. Annular Bodies with Hub

We now turn to the investigation of the influence of circulation for annular bodies with hub. Figures 24 and 25 show the mean camber lines for various velocity conditions in the presence of the thin hub body $R_N/r_0 = 2/3$ once for $a = 0$ and then for $a/r_0 = 1$. In these examples, we investigated only positive circulations ($U_\infty/U_0 \leq 1$) since the

calculations without hub bodies showed, true to expectation, that the outward bending for $U_\infty/U_0 > 1$ is not significant and does not lead to greatly altered bodies.

Figures 24 and 25 indicate the following new effect of the hub body. Since the mean camber line for $U_\infty/U_0 = 1$ now is also curved and narrowed, whereas, the one for $U_\infty/U_0 = 0.2$ has remained practically unchanged compared to its form without the presence of a hub body, these stream surfaces now move considerably closer together. This is particularly noticeable for the position $a/r_0 = 1$. One may assume that this effect will be clearest if the respective streamline has, even without circulation, a form similar to the one in case of a strong circulation. Thus, we are again led to arrangements with a relatively thick hub body in the interior of the cowling - an arrangement found advantageous in other respects as well as in the previous section.

Before investigating such an arrangement, we want to point out the pressure distributions on the mean camber lines shown in figures 24 and 25 (figs. 26 and 27). Their variation is favorably similar to that of the corresponding pressure distributions without hub. In this respect, too, the rearward position $a/r_0 = 1$ appears advantageous among the examples investigated. Figures 28 and 29 show the thick cowlings with hub pertaining to figures 24 and 25. One can see clearly that the separate contours are now considerably less different from each other.

We now investigate the arrangement $R_N/r_0 = 1$ and $a/r_0 = 1$ treated without circulation in the previous section (figs. 12, 18, and 23), for the velocity ratio $U_\infty/U_0 = 0.4$. The mean camber line for ($U_\infty/U_0 = 0.4$ (fig. 30) is shown to differ little from the one for $U_\infty/U_0 = 1$.) In figure 30, the cowlings without circulation with $d/R = 0.2$ and $d/R = 0.12^3$ have been plotted additionally for comparison. One recognizes from figure 30 that for a certain form under various operating conditions, the travel of the stagnation point will not be as extensive as in the absence of a hub body. (Compare fig. 9.) This fact may be explained by a certain guiding of the streamlines by the hub body. This guiding may be additionally aided by a different shaping of the hub body. In regard to the simplicity of the singularities selected, it is, of course, not to be expected that we should have obtained the most favorable forms. The pertaining pressure distributions are shown in figures 31, 32, and 33.

4. Mass Flows and Thrust Forces

So far, we have indicated the velocity ratio U_∞/U_0 as the parameter characteristic for the circulation; however, this makes sense only

³The pertaining pressure distributions may be found in the first report in this series (reference 1).

for our particular selection of infinitely long bodies. We therefore show additionally the connection between U_∞/U_0 and the quantity of fluid Q flowing through the entrance cross section πr_0^2 , for the examples treated, in the following figures 34 to 37. Q_0 there signifies the quantity which would flow through the entrance cross section in the absence of a cowling. With a hub body present, this quantity is smaller than $\pi r_0^2 U_0$ (compare fig. 38). The quantity $Q/\pi r_0^2 U_0$ represents the ratio between mean velocity in the entrance cross section and undisturbed free-stream velocity U_0 , and may be taken from the figures 34 to 37. (Compare also fig. 6.) At this point, it should be mentioned that the thickness of the cowling, too, reduces the mass flow as has been discussed in detail in the first report of this series (reference 1).

Furthermore, we want to investigate what axial forces are absorbed by the entire arrangement and by the cowling, in particular, for the different operating conditions. A detailed calculation by means of the theorem of momentum for the two-dimensional case may be found in P. Ruden's report (reference 3). A corresponding deliberation for our rotationally symmetrical problem leads to a simple formula for the force S exerted by the flow on the total arrangement:

$$S = -\frac{\rho}{2} U_0^2 \pi R^2 \left[1 - \frac{U_\infty}{U_0} \right]^2 \quad (1)$$

According to equation (1), one always obtains a thrust on the combined elements. The component of the force absorbed by the hub may be determined according to A. Betz (reference 4) in a simple manner by presupposing the single source replacing the hub body to be situated so far inside of the cowling that the velocity induced by the vortices and sources of the cowling has, at the locus of the source, already reached the final value

$$u_\infty = \left(\frac{U_\infty}{U_0} - 1 \right) U_0$$

This condition is approximately satisfied shortly behind the entrance opening as has been shown before in section II, 1. The relation

$$S_N = -\rho u_\infty E \quad (2)$$

is then valid for the force at the hub with

$$E = \pi R_N^2 U_\infty$$

signifying the source strength. Therewith S_N becomes

$$S_N = -\frac{\rho}{2} U_o^2 \pi R^2 \left(\frac{R_N}{R}\right)^2 \frac{U_\infty}{U_o} \left(\frac{U_\infty}{U_o} - 1\right) \quad (3)$$

According to this, the hub is subject to a drag for $U_\infty/U_o < 1$, whereas, it takes over part of the total thrust for $U_\infty/U_o > 1$. The axial force S_V at the cowling is obtained as the difference between total thrust and hub force. In figure 39

$$S_V/\frac{\rho}{2} U_o^2 \pi R^2$$

is plotted against U_∞/U_o for various values of R_N/R . One recognizes that the cowling, if it contains a hub body, must, for $U_\infty/U_o < 1$, absorb thrust forces. For

$$U_\infty/U_o > 1 \text{ and } R_N/R \geq \sqrt{1/2}$$

the cowling always experiences a drag which increases with U_∞/U_o . For

$$U_\infty/U_o > 1 \text{ and } R_N/R < \sqrt{1/2}$$

we find at the cowling at first drag, later on, however, again thrust forces.

If the hub is pulled forward so far that at the locus of the single source which replaces it, a velocity stemming from the vortices and sources of the cowling practically no longer exists, the cowling takes over the entire thrust given by equation (1) exactly as in the case where no hub is present.

Since the equations (2) and (3) essentially depend on the selection of the singularities, these relations as well as the figure 39 calculated from them are to be rated only as limiting cases; however, we thus obtain a convenient survey of the forces to be expected. Equation (1) is valid generally with the one presupposition: that the thickness of the cowling for $x \rightarrow \infty$ does not continuously increase.

Finally, we want to point out a problem not yet treated in the present report: that of oblique free-stream direction. Our results apply only to axial free-stream direction. It may, however, be assumed that a slightly oblique direction will not essentially alter the results.

III. SUMMARY

After the statement of the problem and the separate assumptions had been discussed in the first section, the results were represented by a series of examples in the second section. First, the form of the surfaces resulting as stream surfaces for different strength of circulation is determined. The pressure distribution indicated shows that the pressure recovery to a great part takes place ahead of the cowling. The influence of thickness and position of a hub body is represented in the example of bodies without circulation. It is further shown that in the presence of a circulation by suitable selection of thickness and position of the hub body, the cowlings are more similar for the various ratios between internal and external velocity with than without hub body. The body shapes and the pertaining pressure distributions are given for each of the calculated examples. Finally, the axial forces are investigated. The direction of these forces is always opposite to that of the oncoming flow.

Translated by Mary L. Mahler
National Advisory Committee
for Aeronautics

REFERENCES

1. Küchemann, D.: Ueber die Strömung an ringförmigen Verkleidungen endlicher Dicke. (I. Mitteilung). Forschungsbericht Nr. 1236, 1940. (Available as NACA TM 1325.)
2. Küchemann, D.: Tafeln für die Stromfunktion und die Geschwindigkeitskomponenten von Quellring und Wirbelring. Jahrbuch 1940 der Deutschen Luftfahrtforschung, p. I 547.
3. Ruden, P.: Ebene symmetrische Fangdiffusoren. Forschungsbericht Nr. 1209, 1940. (Available as NACA TM 1279.)
4. Betz, A.: Singularitätenverfahren zur Ermittlung der Kräfte und Momente auf Körper in Potentialströmungen. Ing. Archiv Bd. III, 1932, p. 454.

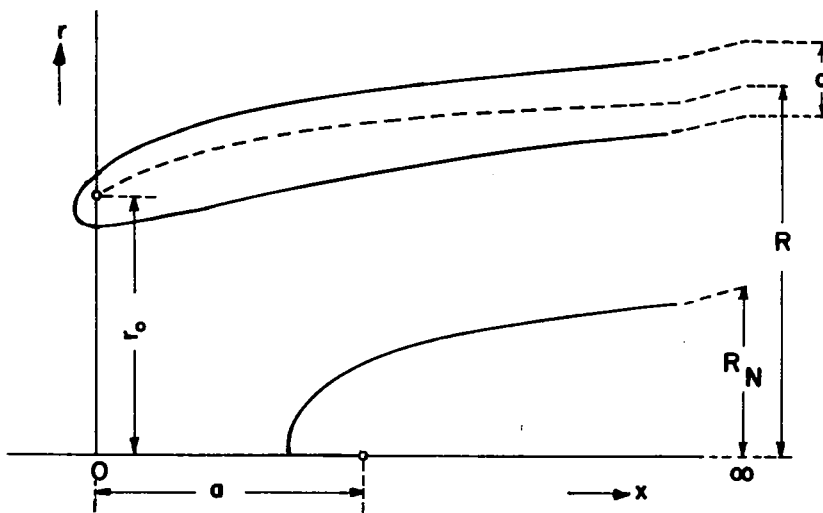


Figure 1.- Over-all sketch for the symbols.

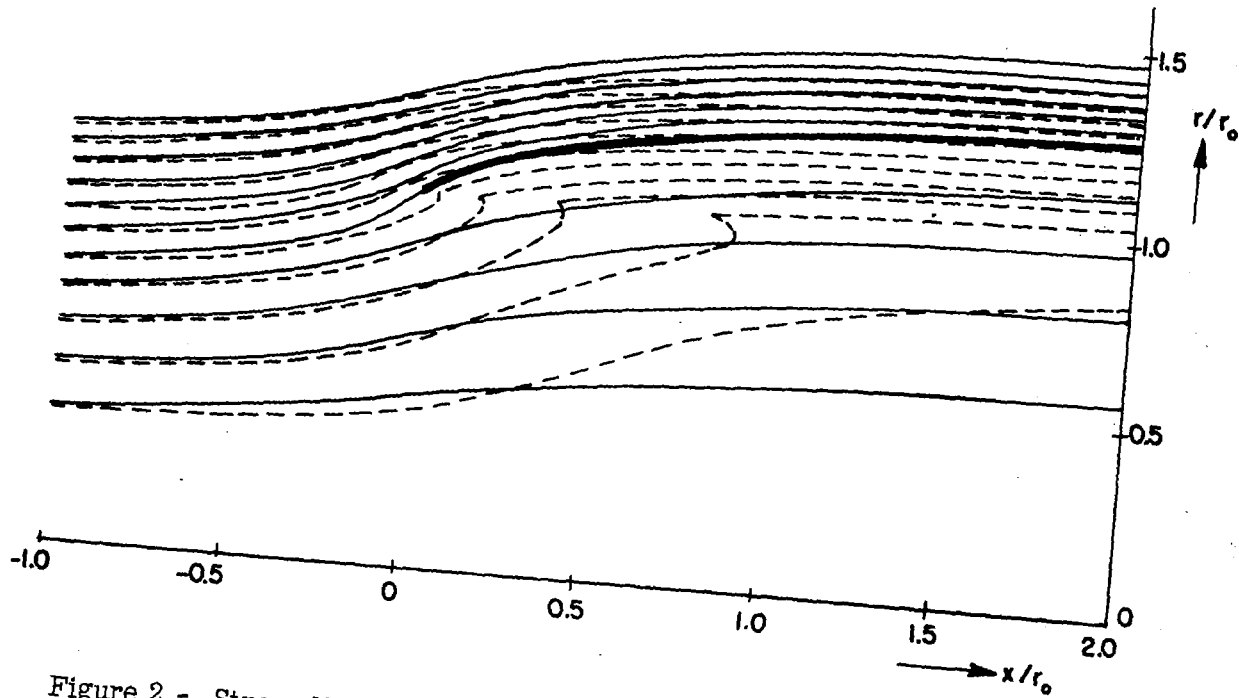


Figure 2.- Streamline pattern. Dashed lines: vortex ring distribution of constant strength in axial direction from $x=0$ to ∞ in a parallel flow. Solid lines: the same distribution on a stream surface which is drawn heavily. U_∞/U_0 about 0.3.

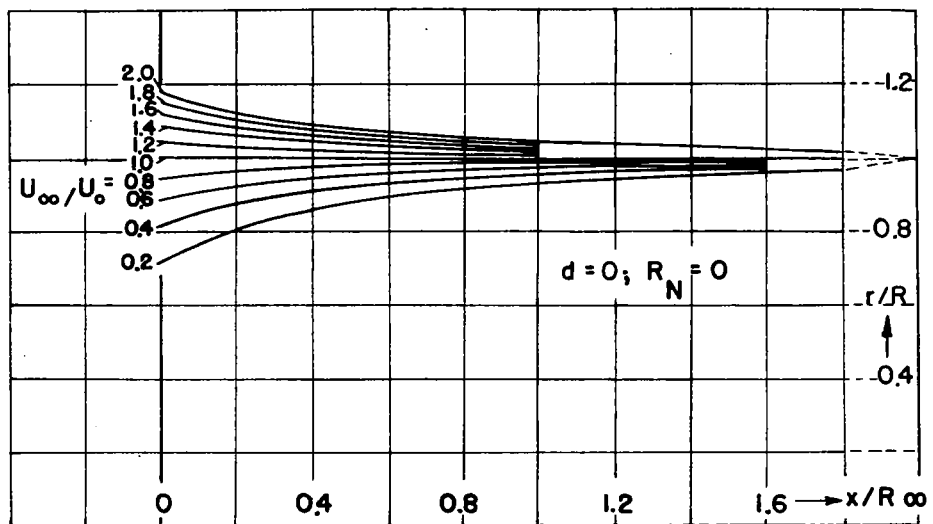


Figure 3.- Distribution stream surfaces for various velocity ratios.

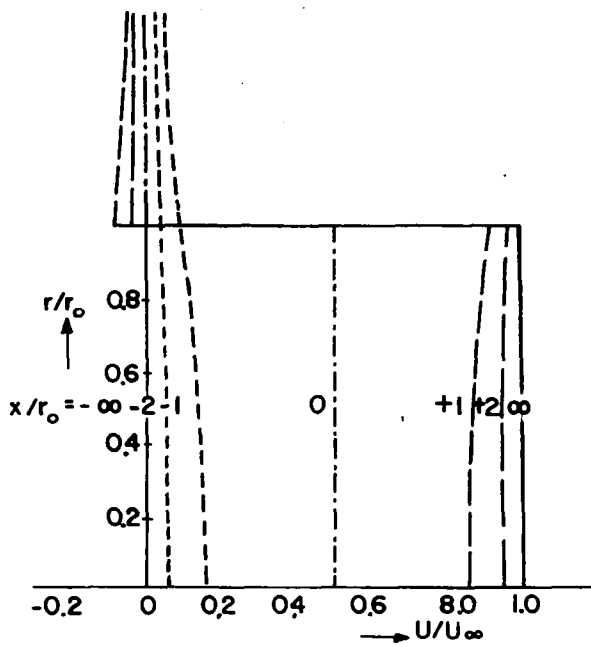


Figure 4.- Axial velocities stemming from a distribution on a circular cylinder in various cross sections.

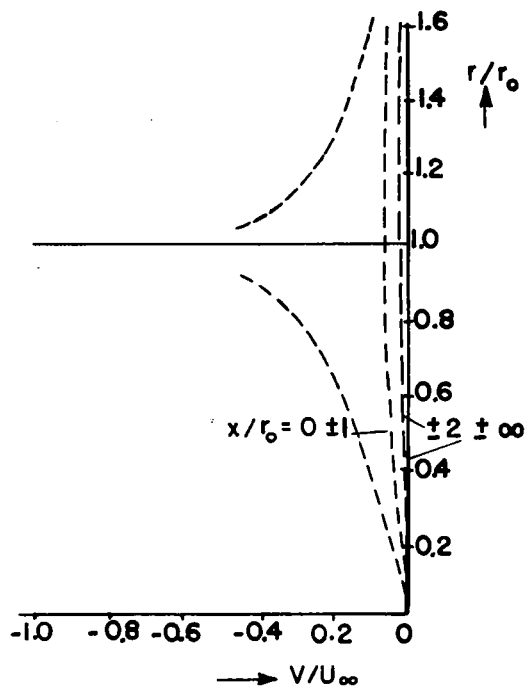


Figure 5.- Radial velocities stemming from a distribution on a circular cylinder in various cross sections.

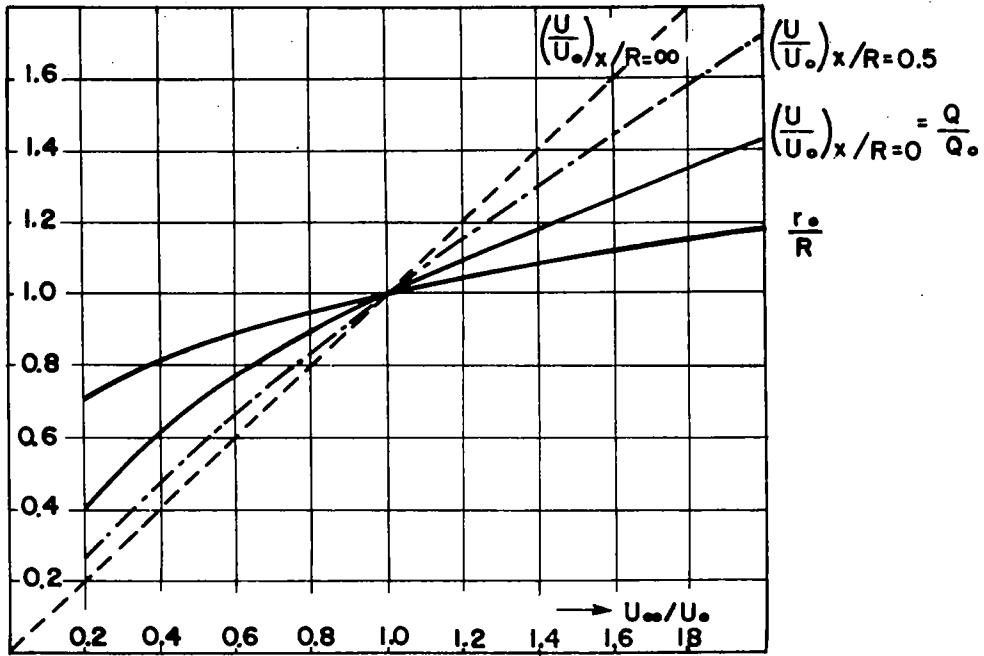


Figure 6.- Mean velocity values, mass flows, and contraction ratios for the distributions shown in figure 3.

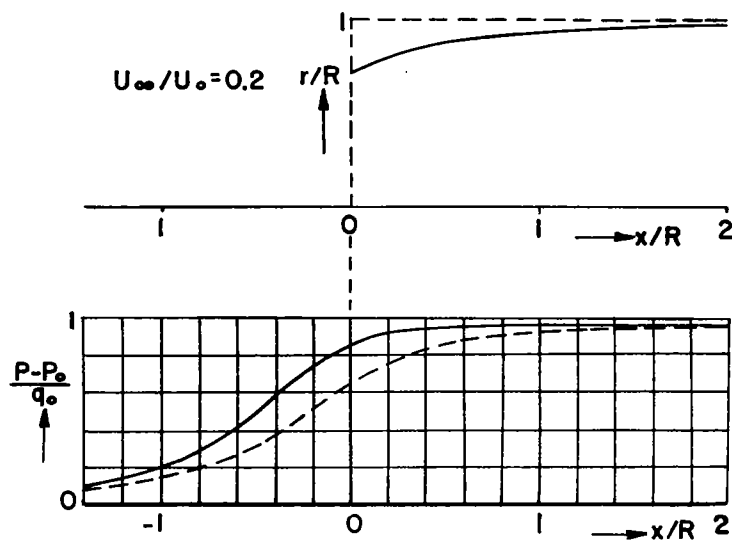


Figure 7.- Pressure distribution on the axis of symmetry for a distribution on a circular cylinder (dashed) and on a stream surface (solid line).

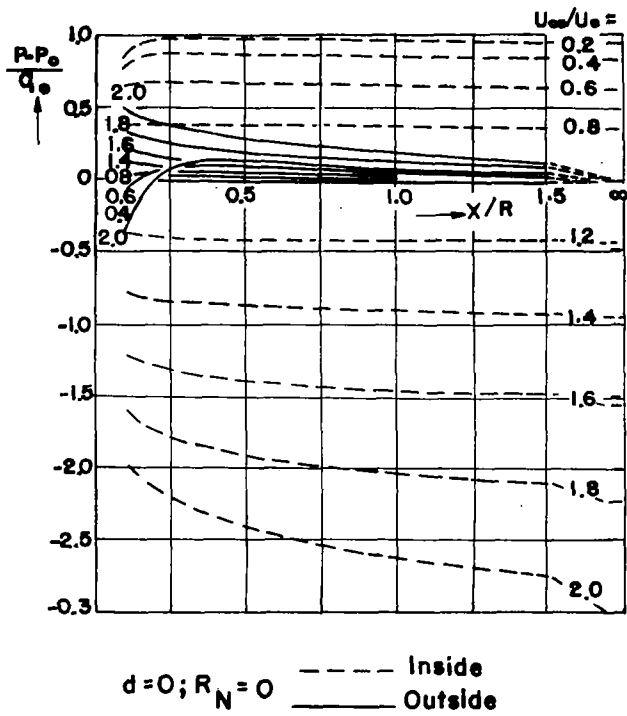


Figure 8.- Pressure distributions on the outside and inside of the distributions shown in figure 3.

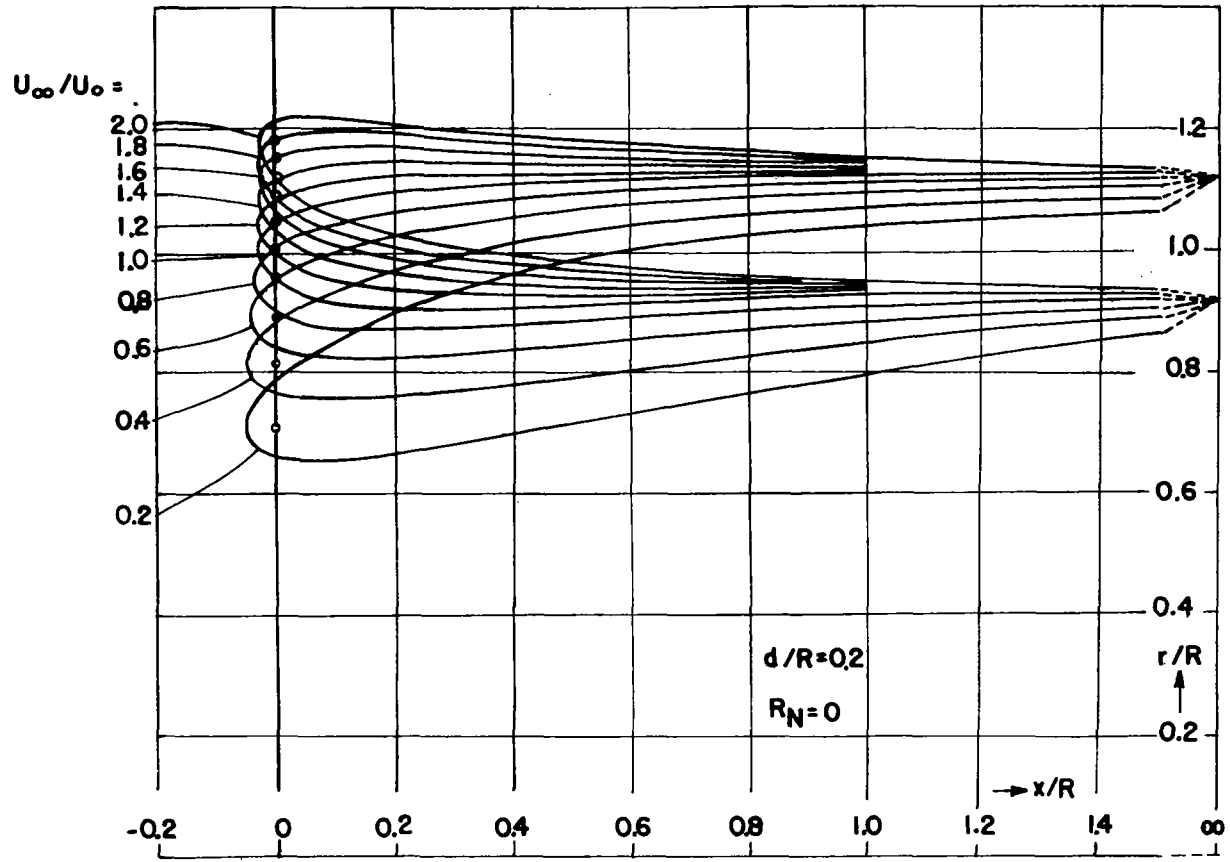


Figure 9.- Contours of annular bodies for various velocity ratios.

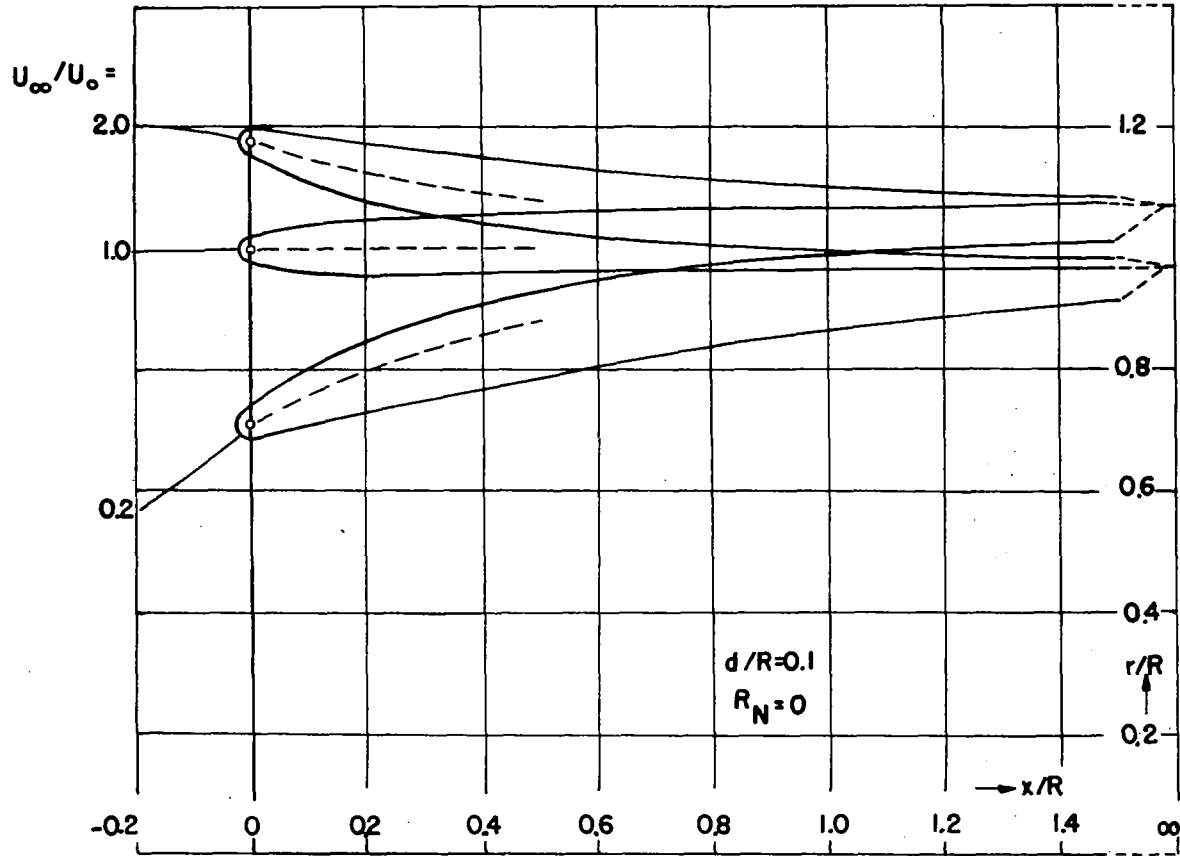


Figure 10.- Contours of annular bodies for various velocity ratios.
Dashed: Mean camber stream surface.

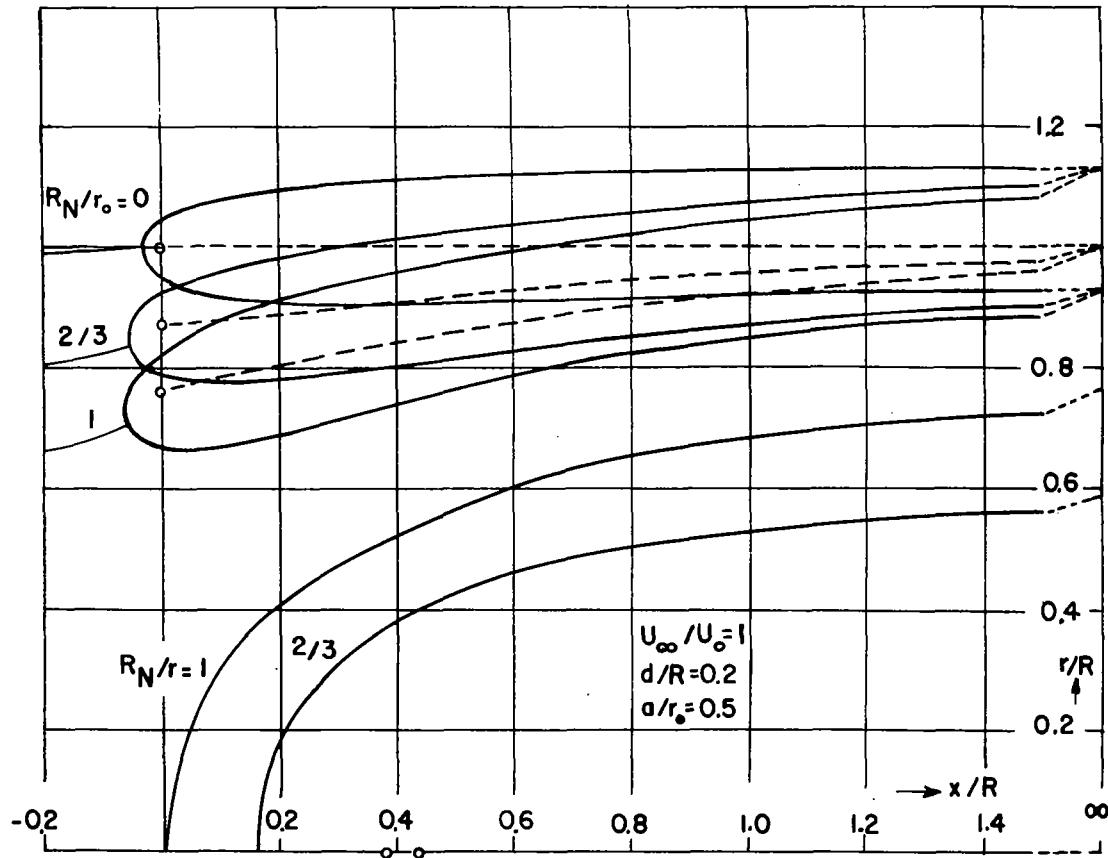


Figure 11.- Contours of annular bodies without circulation for hub bodies of various thickness in $a/r = 0.5$.

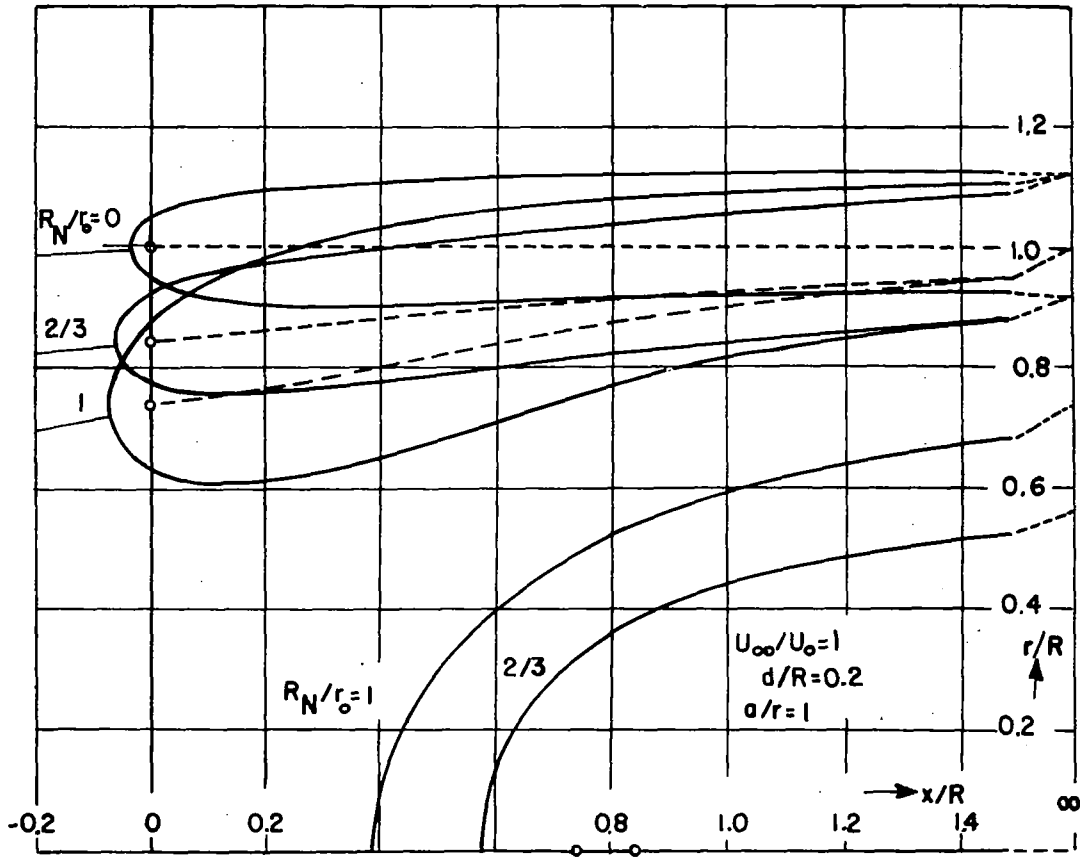


Figure 12.- Contours of annular bodies without circulation for hub bodies of various thickness in $a/r = 1$.

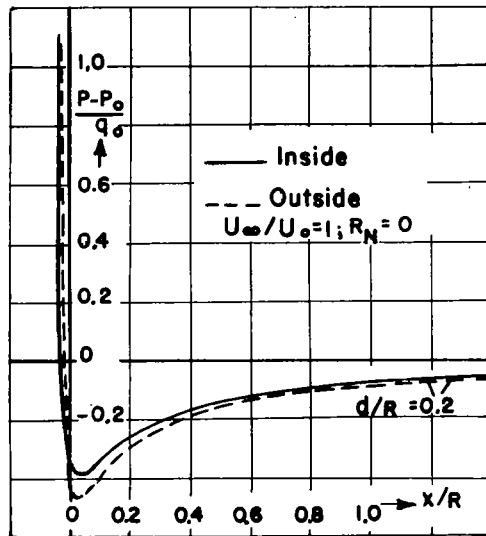


Fig. 13

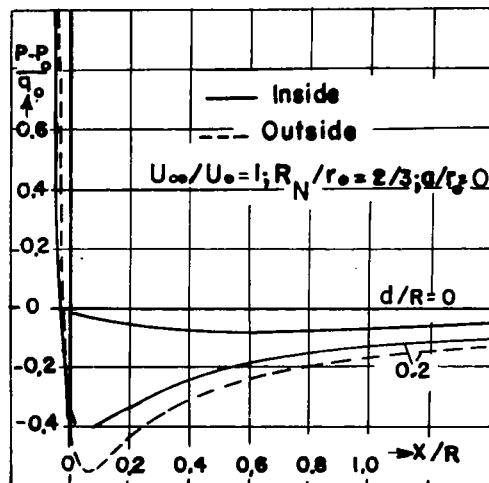


Fig. 14

Figures 13 and 14.- Pressure distributions on the cowlings.

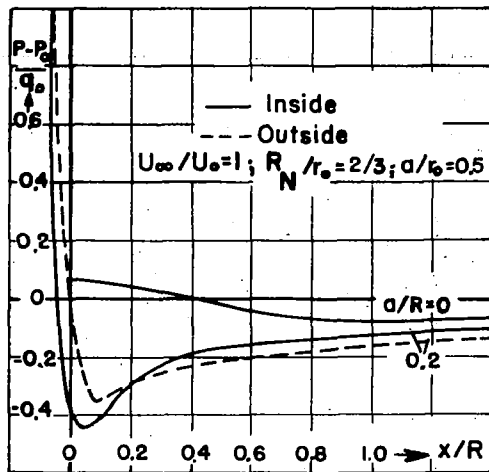


Fig. 15

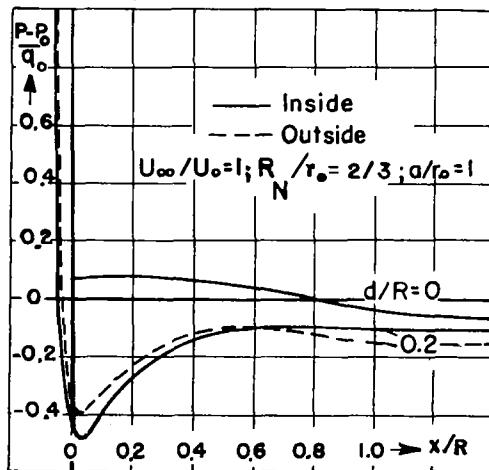


Fig. 16

Figures 15 and 16.- Pressure distributions on the cowlings.

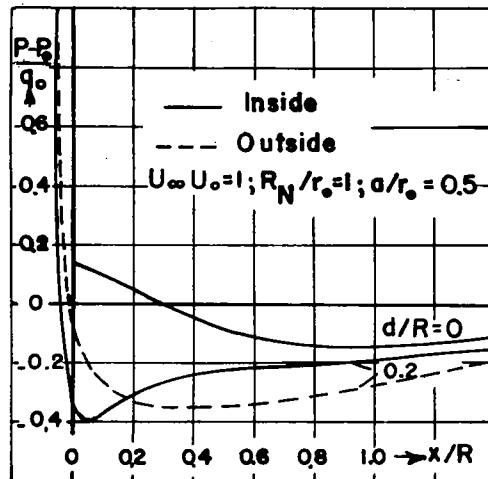


Fig. 17

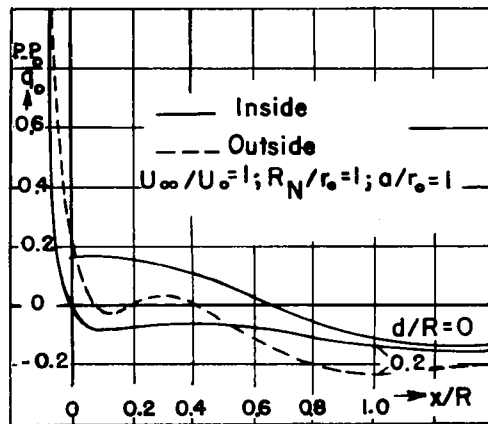


Fig. 18

Figures 17 and 18.- Pressure distributions on the cowlings.

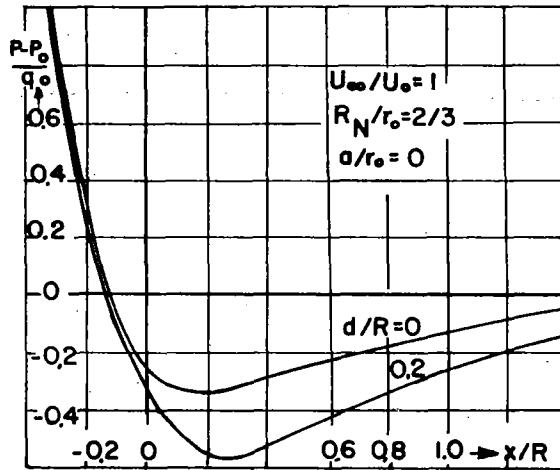


Fig. 19

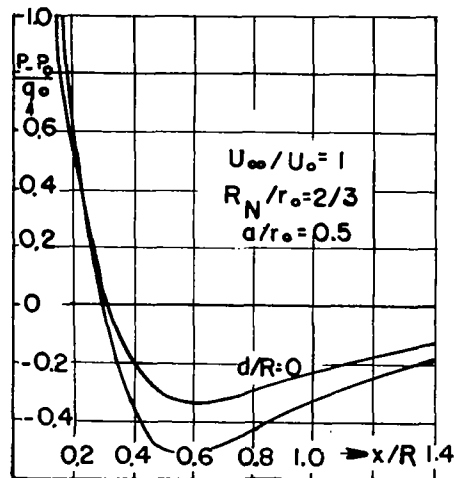


Fig. 20

Figures 19 and 20.- Pressure distributions on the hubs.

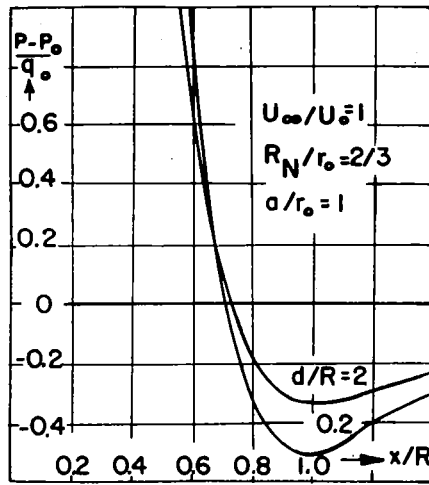


Fig. 21

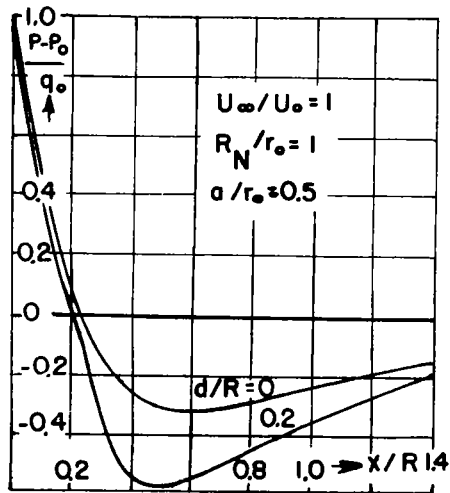


Fig. 22

Figures 21 and 22.- Pressure distributions on the hubs.

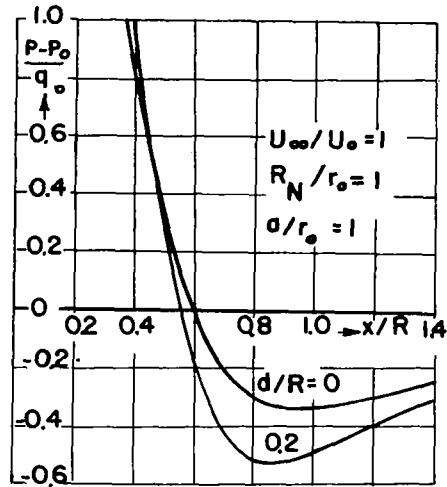


Figure 23.- Pressure distributions on the hubs.

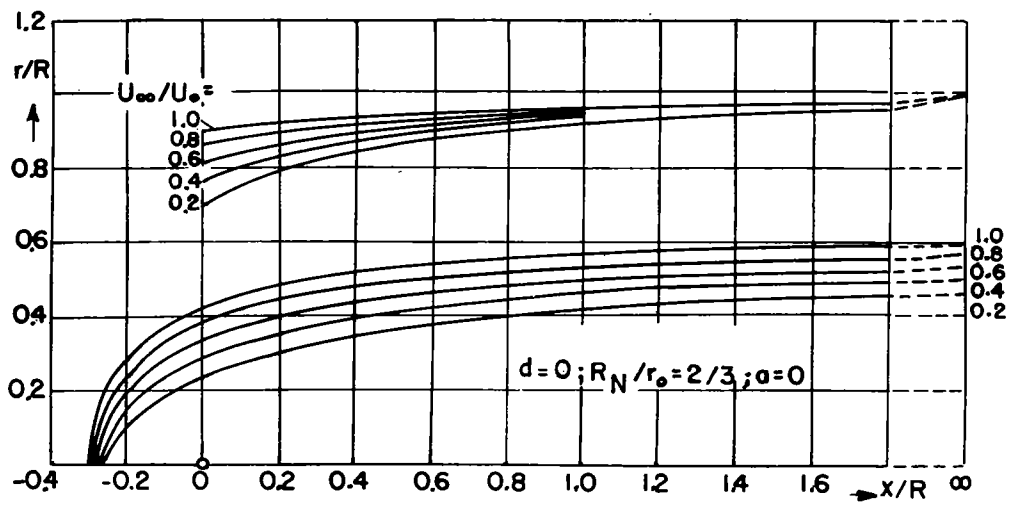


Figure 24.- Mean camber lines and hub bodies for various velocity ratios.

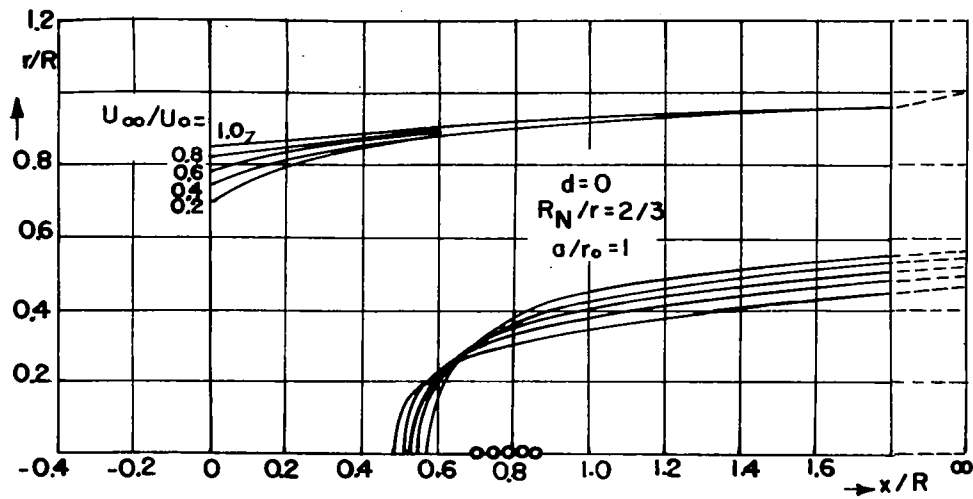


Figure 25.- Mean camber lines and hub bodies for various velocity ratios.

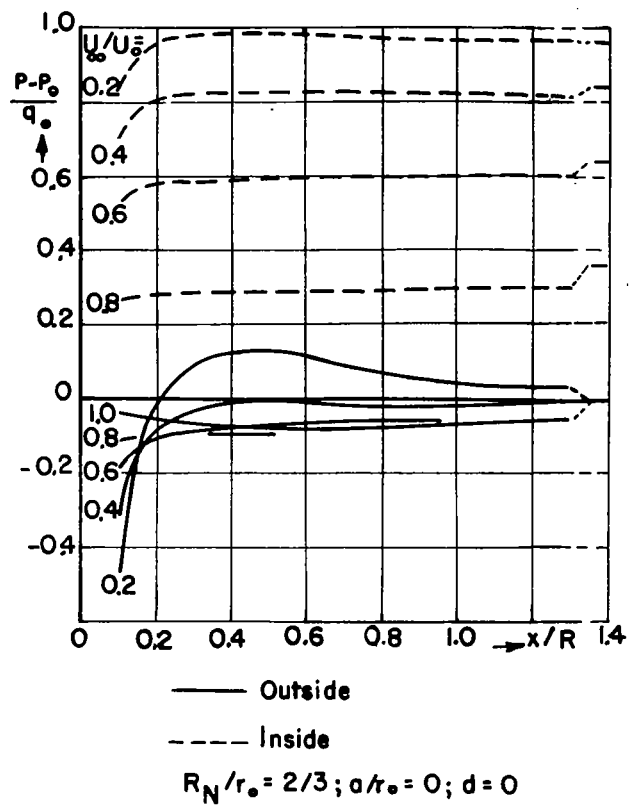


Figure 26.- Pressure distribution on the mean camber lines of figure 24.

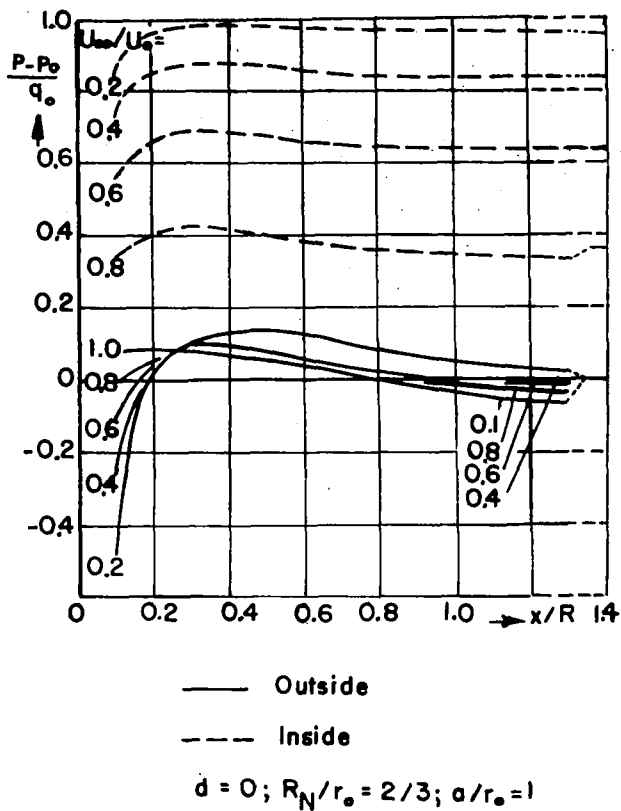


Figure 27.- Pressure distribution on the mean camber lines of figure 25.

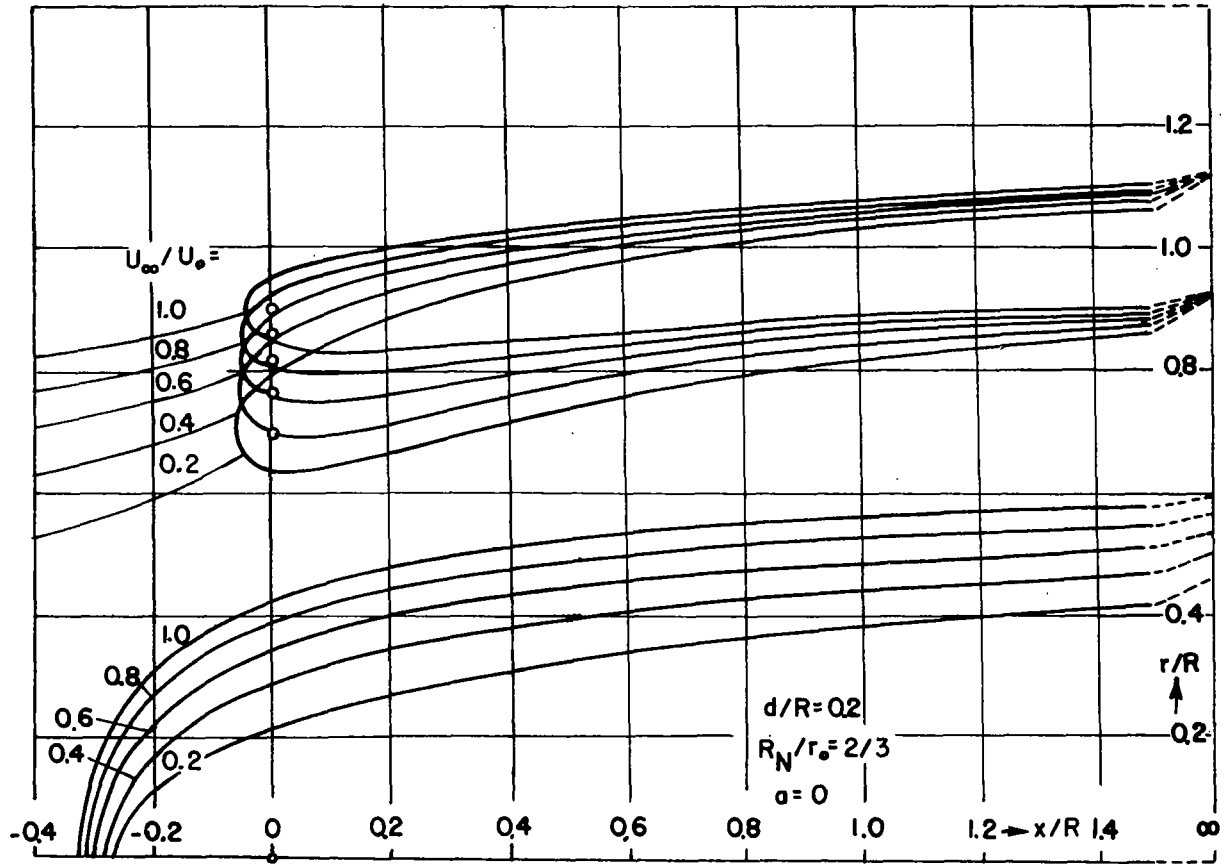


Figure 28.- Contours of annular bodies with hub for various velocity ratios.

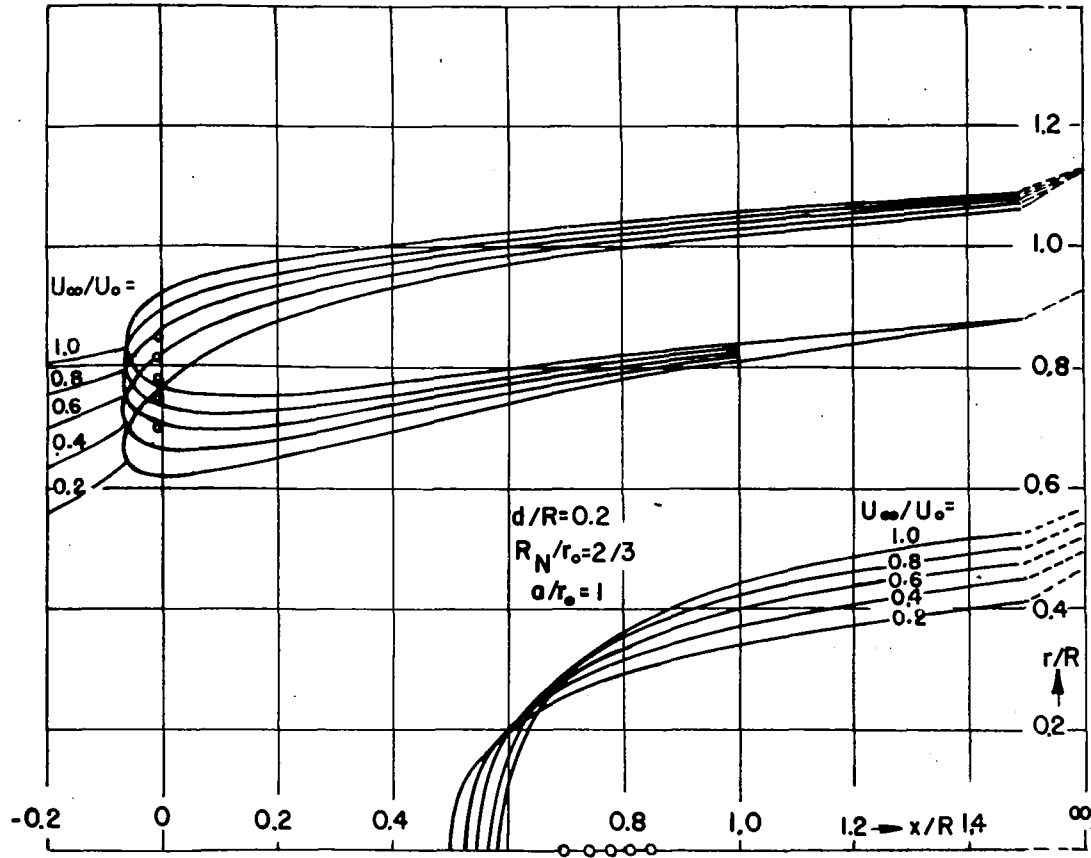


Figure 29.- Contours of annular bodies with hub for various velocity ratios.

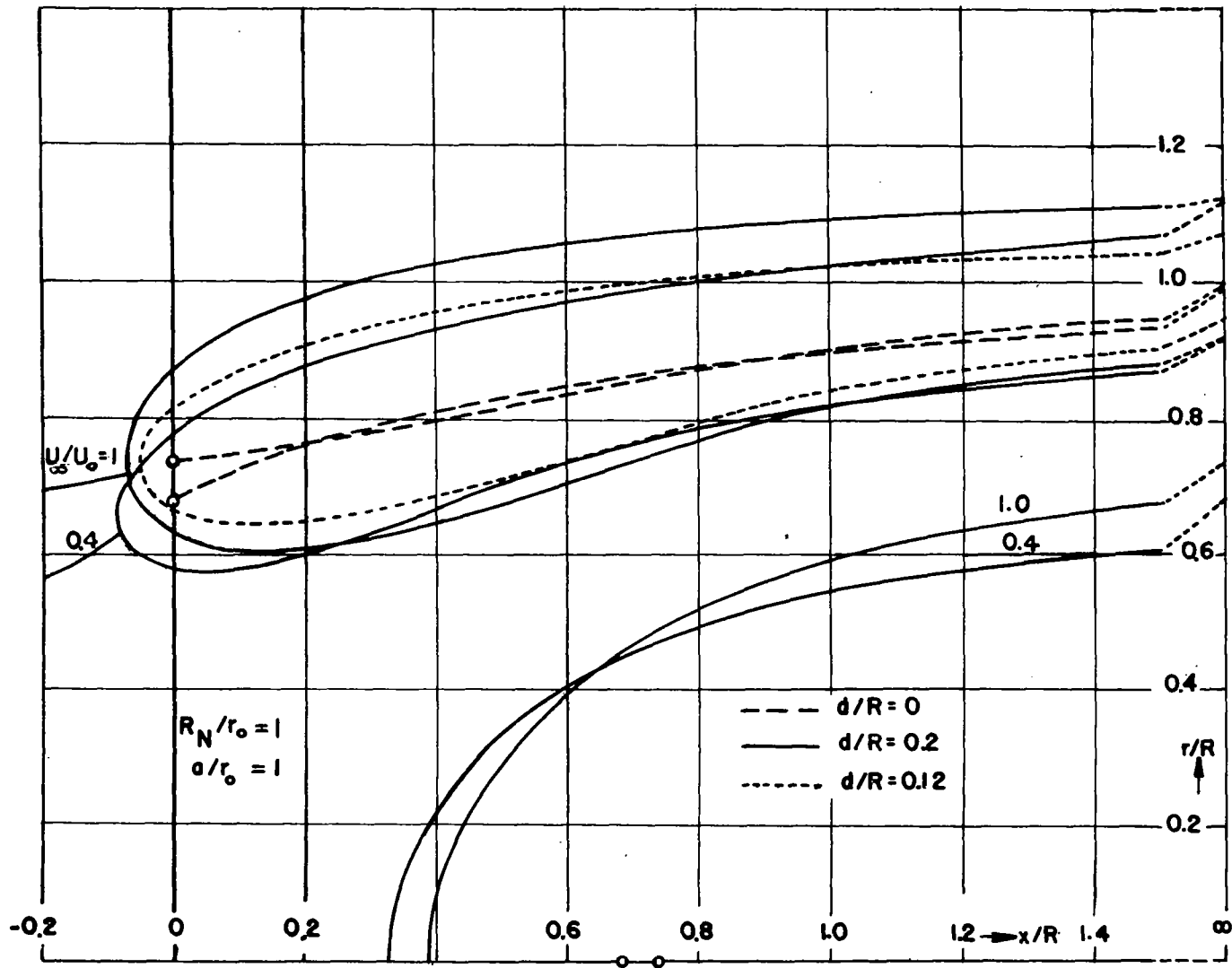
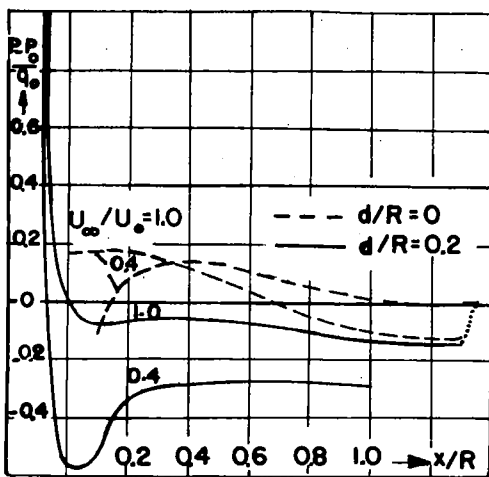


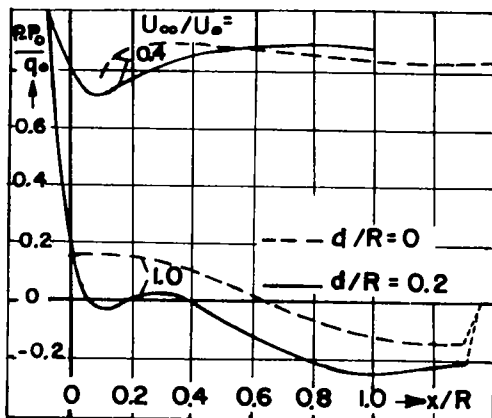
Figure 30.- Contours of annular bodies with hub for various velocity ratios.



Outside

$$R_N/r_0 = 1; a/r_0 = 1$$

Fig. 31



Inside

$$R_N/r_0 = 1; a/r_0 = 1$$

Fig. 32

Figures 31 and 32.- Pressure distributions on the inside of the bodies represented in figure 30.

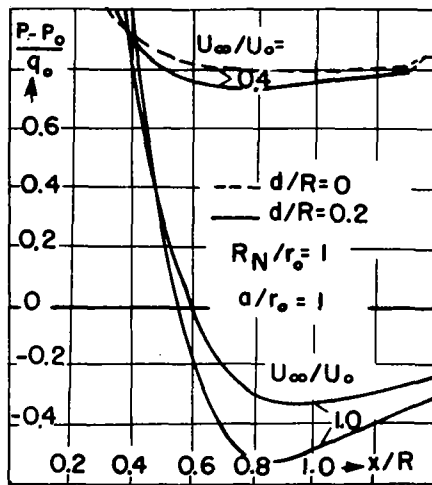


Figure 33.- Pressure distributions on the hub bodies of figure 30.

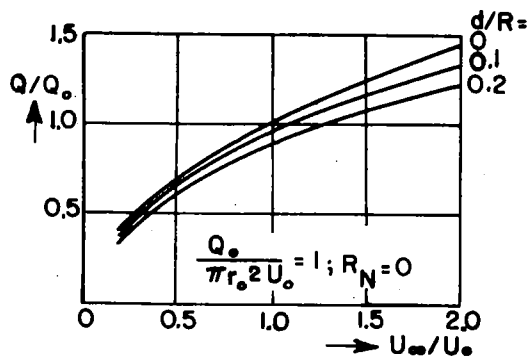


Fig. 34

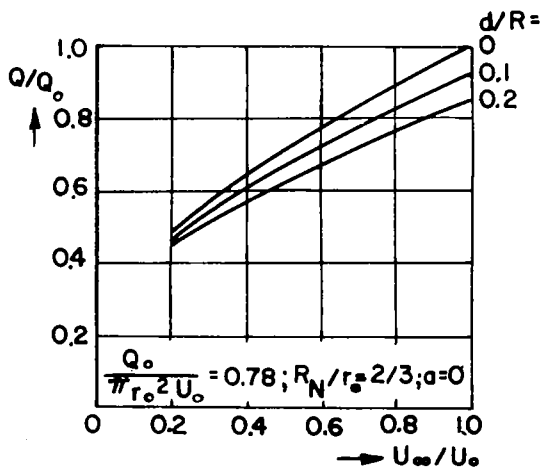


Fig. 35

Figures 34 and 35.- Dependence of the mass flow on the velocity ratio.

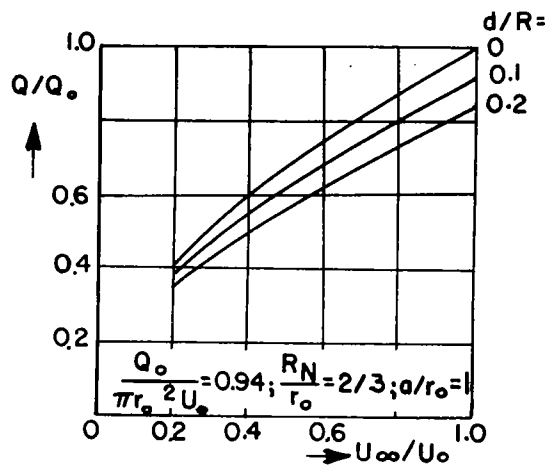


FIG. 36

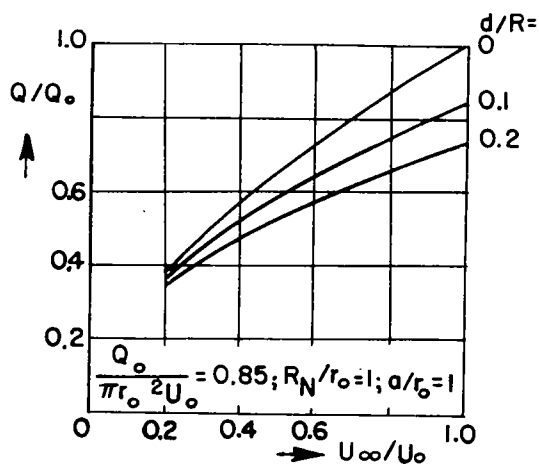


FIG. 37

Figures 36 and 37.- Dependence of the mass flow on the velocity ratio.

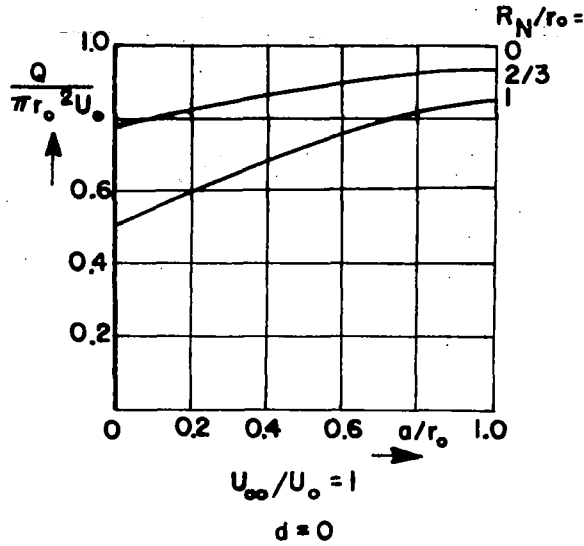


Figure 38.- Dependence of the mass flow on the position and the thickness of the hub body for cowlings without circulation.

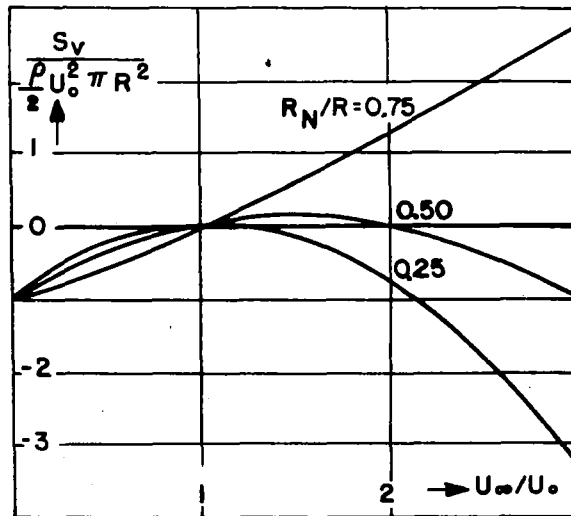


Figure 39.- Thrust coefficient on the cowling as a function of the velocity ratio.

NASA Technical Library



3 1176 01441 2093